Chemical Engineering Journal 147 (2009) 87–96

Contents lists available at ScienceDirect

Chemical Engineering Journal

journal homepage: www.elsevier.com/locate/cej

Kinetics and thermodynamic study of phosphate adsorption on iron hydroxide-eggshell waste

N. Yeddou Mezenner*, A. Bensmaili

Laboratoire de Génie de la réaction, Faculté de Génie Mécanique et Génie des procédés, Université des Sciences et de la Technologie Houari Boumediène, BP 32 El Alia Bab Ezzouar, Alger, Algerie, France

ARTICLE INFO

Article history:
Received 22 March 2008
Received in revised form 25 May 2008
Accepted 21 June 2008

Keywords:
Adsorption
Phosphorus
Kinetics
Modelization
Equilibrium
Thermodynamics

ABSTRACT

This study explored the feasibility of using waste iron hydroxide-eggshell as adsorbent for the removal of phosphate under different experimental conditions. In our experiments, the batch sorption is studied with respect to solute concentration (2.8–110 mg/L), contact time, adsorbent dose (2.5–20 g/L) and solution temperature (20–45 °C). The Langmuir, Freundlich, and Langmuir–Freundlich adsorption models were applied to experimental equilibrium data at different solution temperatures and the isotherm constants were calculated using linear regression analysis. A comparison of kinetic models applied to the adsorption of phosphate onto iron hydroxide-eggshell was evaluated for the pseudo-second-order, Elovich, intra-particle diffusion and Bangham's kinetics models. The experimental data fitted very well the pseudo-second-order kinetic model and also followed by intra-particle diffusion model up to 5 min, whereas diffusion is not only the rate-controlling step. The results show that the sorption capacity increases with an increase in solution temperature from 20 to 45 °C at the initial phosphate solution concentration of 27 mg/L. The thermodynamics parameters were evaluated. The positive value of ΔH° (81.84 kJ/mol) indicated that the adsorption of phosphate onto iron hydroxide-eggshell was endothermic, which result was supported by the increasing adsorption of phosphate with temperature. The positive value of ΔS° (0.282 kJ/mol) reflects good affinity of phosphate ions towards the waste iron hydroxide-eggshell. The results have established good potentiality for the waste iron hydroxide-eggshell particles to be used as a sorbent for the removal of phosphorus from wastewater.

1. Introduction

Phosphorus exists in natural waters in particulate and dissolved form. It is known that phosphorus is essential to the growth of algal and other biological organisms. Because of algal blooms that occur in surface waters, the amount of phosphorus compounds in domestic and industrial discharges must be controlled using either chemical or biological techniques. The usual forms of phosphorus found in aqueous solutions include orthophosphates, polyphosphates and organic phosphates [1]. The principal phosphorus compounds in wastewater are generally orthophosphates [2]. Municipal wastewater may contain from 4 to 15 mg/L phosphorus as PO_4^{3-}. However, industrial wastewaters (such as detergent manufacturing and metal coating processes) may contain phosphate levels well in excess of 10 mg/L [3]. Chemical treatment is widely used for phosphate removal. Chemicals such as lime, alum, and Ferric chloride are the common precipitants used for phosphate removal [4] but their cost and sludge production make chemical treatment an unattractive option for wastewater treatments. Sorption method can remove phosphate steadily. In recent years, considerable attention has been paid on economic and environmental concerns to the study of using different types of low-cost sorbents such as alum sludge [5] red mud [6], fly ash [7], blast furnace slag [8], spent alum sludge [9], aluminium and iron-rich residues [10], synthetic boehmites [11] and calcite [12].

The objective of this work was to study the feasibility of using hydroxide-eggshell as an adsorbent for phosphorus removal from wastewater. It is well known that calcite [12] and iron oxides are the important phosphorus adsorbent [13]. Eggshell is composed mainly of calcium carbonate which should behave as known sorbents that contain this compound, i.e. calcite [14] calcareous soil [15].

The objective of this work was to study the feasibility of using iron hydroxide-eggshell as an adsorbent for phosphate species removal from wastewater. In doing so, the adsorption of phosphate on this waste material from aqueous solutions was evaluated in batch experiments. The adsorption isotherms, kinetics and temperature effect were studied.

* Corresponding author. Fax: +33 213021247169.
E-mail addresses: yeddouna@yahoo.fr, mezennerna@yahoo.fr (N.Y. Mezenner).

1385-8947/$ – see front matter © 2008 Elsevier B.V. All rights reserved.
doi:10.1016/j.cej.2008.06.024

Table 1
Chemical components of eggshell

Component	%
Na_2O	0.489
MgO	0.845
Al_2O_3	0.055
SiO_2	0.010
P_2O_5	0.181
SO_3	0.747
K_2O	0.050
$CaCO_3$	97.015
Fe_2O_3	0.029
SrO	0.140
Cl	0.138
Volatile matter	0.300

2. Experimental

2.1. Materials and methods

2.1.1. Adsorbent

Our previous study [16] explored the feasibility of utilizing waste eggshell as adsorbent for iron removal from aqueous solution, then, the waste (iron hydroxide-eggshell) derived from adsorption process of iron into eggshell was used for adsorption of phosphate species in this work. The chemical composition of eggshell is summarized in Table 1; values are expressed as % (w/w).

For the preparation of iron hydroxide-eggshell, solution of 5 mg/L Fe (III) was prepared by dissolving ($FeCl_3$, $2H_2O$) in distilled water. 0.25 g sample of eggshell were added to each 100 mL of 5 mg/L Fe (III) (several samples were prepared). The mixture was agitated on shaker at a constant temperature at equilibrium. Then, the samples were centrifuged and the adsorption amount on eggshell was calculated indirectly from the difference of iron concentration in solution before and after the experiment [16]. Waste (iron hydroxide-eggshell) resulting in each sample contain 1.99 mgFe (III) adsorbed per unit mass of eggshell (~2 mgFe (III)/g). The sorbent was dried, screened through a set of sieves to get a geometrical size of 50–315 μm and used for phosphate removal.

2.1.2. Absorbate

Stock solutions were prepared by dissolving accurately weighed samples of anhydrous potassium phosphate (KH_2PO_4) in distilled water to give a concentration of 1000 mg/L and diluted with distilled water when necessary.

2.2. Kinetic studies

The iron hydroxide-eggshell mass (7.5 g/L), except for the studies of adsorbent concentration effect, was mixed with 1000 mL of the desired phosphate concentration and temperature in conical flasks. Initial pH of each solution was adjusted to the required value (pH 7) with diluted NaOH solutions before mixing the adsorbent solution. The flasks were agitated on a shaker at constant temperature. Samples were withdrawn at suitable intervals and were separated from the sorbent by centrifugation for 20 min. The phosphate concentration was determined by measuring the absorbance of the solution using UV visible at 880 nm wavelength after the samples were pre-treated using the ascorbic acid method [17]. Experiments were repeated for different initial phosphate concentration (2.8, 14, 53 and 110 mg/L) and temperature (20, 25, 35 and 45 °C) values.

2.3. Equilibrium studies

2.3.1. Effect of adsorbent dose

Adsorption equilibrium studies were conducted at initial phosphate solution pH of 7. Equilibrium data were obtained by adding 0.25–2.0 g of iron hydroxide-eggshell into a series of conical flasks each filled with 100 mL of phosphate solution. The initial phosphate concentration ranges from 14 to 53 mg/L. The conical flasks then covered with aluminium foil and were then placed in a thermostatic shaker for 4 h. During the adsorption the temperature of system was kept constant at 45 °C.

2.3.2. Sorption isotherms

Adsorption experiments were carried out by adding a fixed amount of adsorbent (0.75 g) to a series of conical flasks filled with 100 mL diluted solutions (7–140 mg/L). The conical flasks were placed in a thermostatic shaker at 20, 25, 35 and 45 °C at pH 7.

The removal efficiency (E) of phosphate on iron hydroxide-eggshell, the sorption capacity, (q) and distribution ratio (K_d) were calculated from Eqs. (1)–(3):

$$E(\%) = \frac{C_i - C_f}{C_i} \times 100 \quad (1)$$

$$q = \frac{V(C_i - C_f)}{m} \quad (2)$$

$$K_d = \frac{\text{amount of phosphate in adsorbent}}{\text{amount of phosphate in solution}} \times \frac{V}{m}\,(\text{L/g}) \quad (3)$$

where C_i and C_f are the initial and final concentrations of phosphate (mg/L) in aqueous solution, respectively, V is the volume of the solution (L) and m represents the weight of the adsorbent (g).

3. Results and discussion

3.1. Effect of initial phosphate concentration and contact time

Experiments were undertaken to study the effect of varying initial concentration (2.8–110 mg/L) at 30 °C on phosphate removal by iron hydroxide-eggshell. Fig. 1 indicates a rapid initial uptake rate of phosphate at the beginning and, thereafter, the adsorption rate decreased gradually. The adsorption of phosphate reached

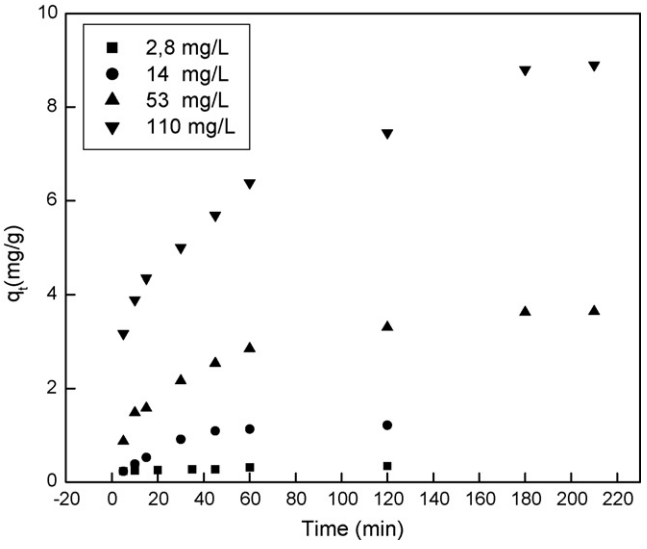

Fig. 1. Effect of contact time at several initial phosphate concentration on sorption kinetics (30 °C, pH 7, C_s = 7.5 g/L).

equilibrium at variable time according to the initial concentration of phosphate: about 60 min (C_i = 2.8 mg/L), 220 min (14, 53 and 110 mg/L). The higher the initial concentration of phosphate species, the larger is the amount of phosphate species adsorbed. The increase in uptake capacity of the sorbent with increasing phosphate concentration may be due to the increase of sorbate quantity. The variation in the extent of adsorption may also be due to the fact that initially all sites on the surface of sorbent were vacant and the solute concentration gradient was relatively high. Consequently, the extent of phosphate species uptake decreases significantly with the increase of contact time, which is dependent on the decrease in the number of vacant sites on the surface of iron hydroxide-eggshell. Besides, after lapse of some time, the remaining vacant surface sites are difficult to be occupied due to repulsive forces between the solute molecules on the solid surface and the bulk phase. Generally, when adsorption involves a surface reaction process, the initial adsorption is rapid. Then, as lower adsorption would follow, as the availed adsorption site gradually decreases, which is consistent with studies reported before [18].

It was observed from Fig. 2 that the percentage of removal decreased with increased initial phosphate concentration from 95% for 2.8 mg/L phosphate to 64% for 110 mg/L phosphate. The lower uptake at higher concentration resulted from an increased ratio of initial number of moles of phosphate to the available surface area; hence fractional adsorption becomes dependent on initial concentration. For a given adsorbent dose the total number of available adsorption sites is fixed thereby adsorbing almost the same amount of adsorbate, thus resulting in a decrease in the percentage removal of the adsorbate corresponding to an increase in initial adsorbate concentration. Similar results were also reported for the adsorption of phosphates from aqueous solution onto fly ash [19].

3.2. Effect of sorbent dosage

The sorbent concentration is another factor that influences the sorption equilibrium. In order to examine the effect of the sorbent dosage on the removal efficiency phosphate, adsorption experiments were set up with various amounts of dried iron hydroxide-eggshell (0.25, 0.5, 0.75, 1.0, 1.5, 2.0 g/100 mL) and phosphate concentrations (14, 27, 53 mg/L). The effect of sorbent dosages on the percentage removal of phosphate has been shown in Fig. 3. It followed the predicted pattern of increasing percentage sorption as the dosage was increased and reaches a saturation level at high doses. For the range of phosphate concentrations examined here, 10 g/L of adsorbent was observed to be the upper limit for the removal of phosphate. This is probably because of the resistance to mass transfer of phosphate from bulk liquid to the surface of the solid, which becomes important at high adsorbent loading in the conical flask in which the experiment was conducted. Moreover, the percentage removal was decreased slightly with the higher dosage (>10 g/L). It might have happened that the higher dose causes particles aggregates and interference or repulsive forces between binding sites, therefore decrease the interaction of phosphate ions with the sorbent and reduces the total surface area of the adsorbent.

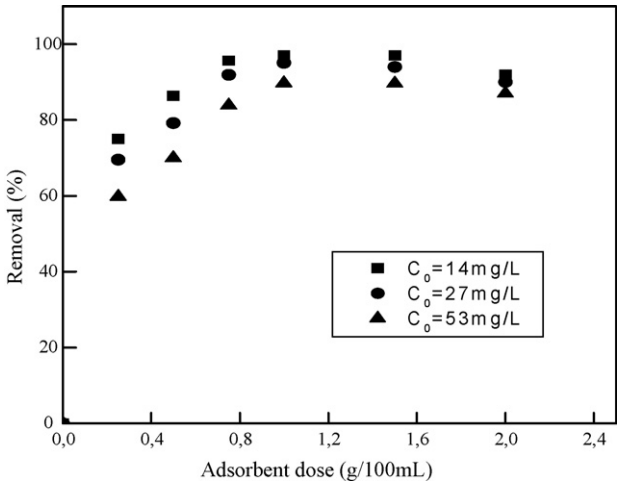

Fig. 3. Effect of adsorbent dosage on phosphate removal (45 °C, pH 7).

3.3. Effect of temperature

The effect of temperature on phosphate uptake capacity (q_e) of iron hydroxide-eggshell was studied. From Fig. 4, it was observed that the phosphate uptake capacity (q_e) of iron hydroxide-eggshell increased with increasing temperature up to 45 °C, indicating that the adsorption of phosphate ions was favoured at higher temperatures. The sorption of phosphate is endothermic, thus the extent of

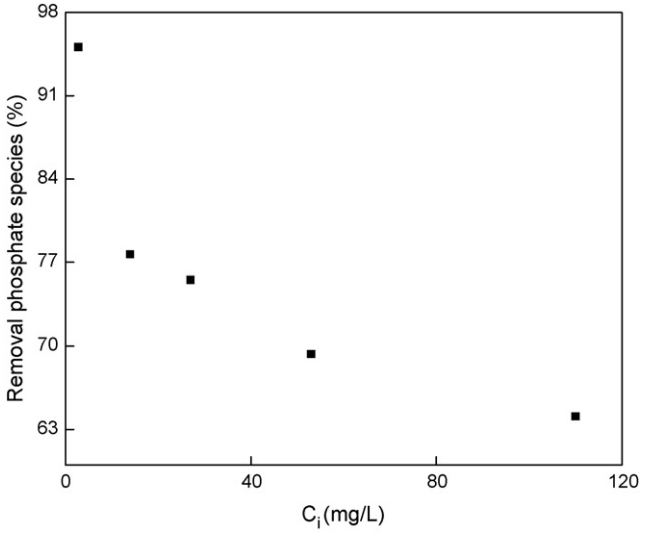

Fig. 2. Effect of initial concentration of phosphate ions in the solution on sorption kinetics (30 °C, pH 7, C_s = 7.5 g/L).

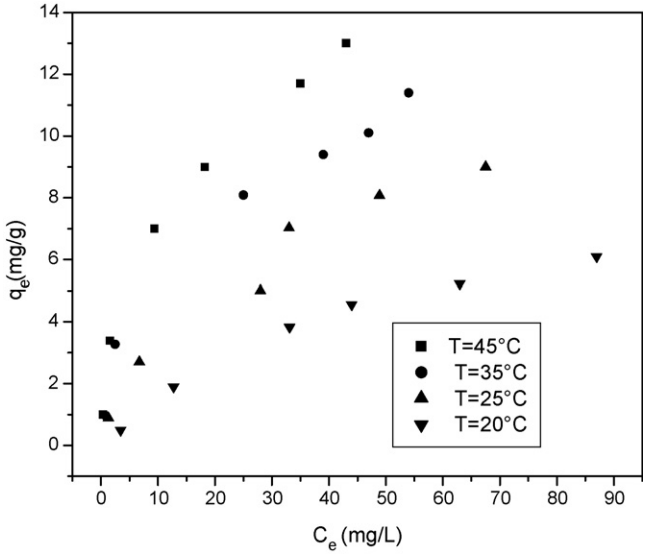

Fig. 4. Phosphate adsorption on iron hydroxide-eggshell at various temperatures.

adsorption increased with increasing temperature. The sorption of phosphate by iron hydroxide eggshell may involve not only physical but also chemical sorption. This result may be due to increased solubility of iron-eggshell compound providing more iron and calcium hydrolysis complexes for phosphate precipitation with an increase in the solution temperature; similar trend was also observed for phosphate removal using raw and activated red mud and fly ash as adsorbent [20].

3.4. Modelling of the sorption equilibrium depending on temperature

In order to optimize the design of a sorption system to remove phosphate from aqueous solutions, it is important to establish the most appropriate correlation for the equilibrium curves. The isotherms data were analyzed using three of the most commonly used equilibrium models, Langmuir [21], Freundlich [22] and Langmuir–Freundlich (Sips) [23]. The mathematical expressions are given by Eqs. (4)–(6), respectively, as follows:

$$q_e = q_{max}\frac{bC_e}{1+bC_e} \quad (4)$$

$$q_e = K_f.C_e^{1/n} \quad (5)$$

$$q_e = q_{max}\frac{C_e^{\beta}}{K+C_e^{\beta}} \quad (6)$$

where q_{max} (mg/g), is the maximum amount of sorbate per unit weight of adsorbent, to form a complete monolayer on the surface bound at high C_e, and b (L/mg) is a constant related to the affinity of the binding sites. q_m and b can be determined from the linear plot of C_e/q_e versus C_e.

K_f and n are the Freundlich constants characteristics of the system (n dimensionless; K_f (mg $L^{-1/n}$ g^{-1} $L^{1/n}$)). Eq. (5) can be linearized in logarithmic form and the Freundlich constants can then be determined.

The generalized adsorption isotherm has been used in linear form. A plot of the equilibrium data in form of $\ln[(q_{max}/q_e)-1]$ versus $\ln C_e$ gives isotherm constants, K is the saturation constant (mg/L); β is the cooperative binding constant; q_{max} is the maximum adsorption capacity of the adsorbent (mg/g). The adsorption isotherms for phosphate ions on iron hydroxide-eggshell at different temperatures are presented in Fig. 4. Figs. 5–7 show the plots of the linearized form. The Langmuir model is an ideal model for homogeneous monolayer adsorption while the Langmuir–Freundlich model is obtained by introducing a power-law expression of the Freundlich model into the Langmuir model. Not that the Langmuir–Freundlich model reduces to the Langmuir form when $n = 1$. The best-fit values of the model parameters estimated from Eqs. (4)–(6) by linear regression analyses are listed in Table 2. Also are shown the correlation coefficients (r^2), which provide measure of model fitness.

A comparison of the experimental isotherms with the adsorption isotherm models showed that the Langmuir equation represented the poorest fit of experimental data ($r^2 = 0.9373$) at 20 °C as compared to the other isotherm equations. It has been found that the best fitted isotherm equations at 35 °C were Langmuir and generalized isotherm with $r^2 \geq 0.9848$. The n parameter of the Freundlich equation ($1.167 < n < 1.940$) reveals adsorption sites with low energetically heterogeneity of this natural adsorbent [24]. Both K_f and n reached their corresponding maximum values, at 45 °C. This implies that binding capacity reaches the highest value and the affinity between the sorbent and phosphate ions was also higher than other temperature values investigated (Table 2). The constant b represents affinity between the sorbent and sorbate,

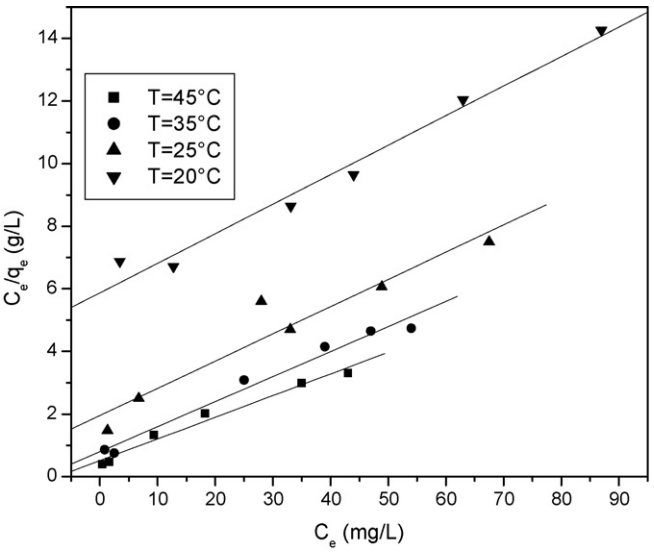

Fig. 5. Langmuir adsorption isotherm for phosphate on iron hydroxide-eggshell at various temperatures.

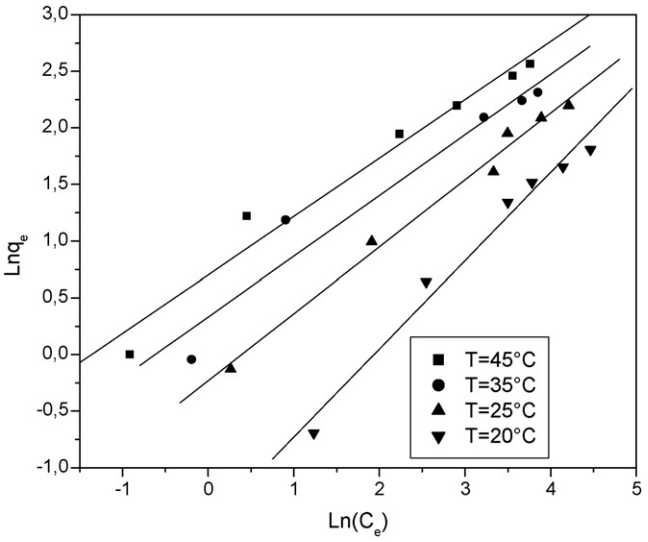

Fig. 6. Freundlich adsorption isotherm for phosphate on iron hydroxide-eggshell at various temperatures.

Table 2
Isotherm constants for phosphate adsorption onto iron hydroxide-eggshell

Parameters	Temperature			
	45 °C	35 °C	25 °C	20 °C
Freundlich				
n	1.94	1.867	1.284	1.167
K_f (mg $L^{-1/n}$ g^{-1} $L^{1/n}$)	2.017	1.39	0.22	0.187
r^2	0.9674	0.9450	0.9771	0.9743
Langmuir				
q_{max} (mg/g)	14.49 12.51	11.49	10.60	
b (L/mg)	0.135	0.10	0.044	0.016
r^2	0.9774	0.9924	0.9237	0.9373
Generalized isotherm				
β	0.924	0.9887	0.9279	1.021
K (mg/L)	6.0131	7.95	17.64	66.68
r^2	0.9629	0.9848	0.9659	0.9968

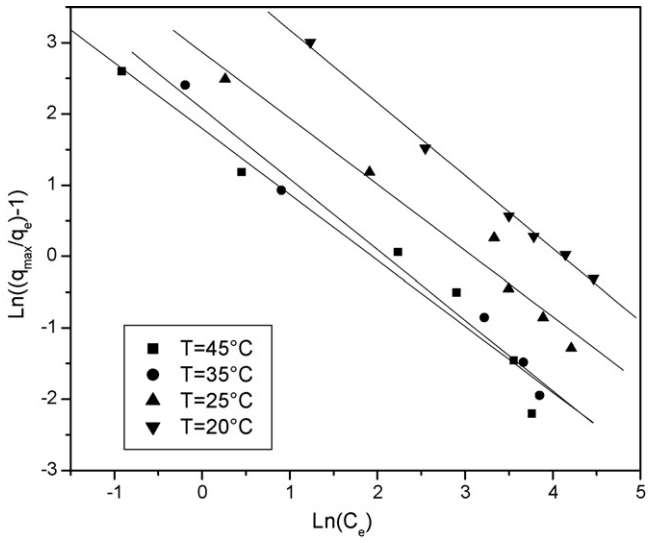

Fig. 7. Langmuir–Freundlich adsorption isotherm for phosphate on iron hydroxide-eggshell at various temperatures.

both q_{max} and b increases from 10.60 to 14.49 mg/g and from 0.016 to 0.135 L/g respectively with increasing Temperature from 20 to 45 °C. The correlation coefficient of Langmuir isotherm equation ($r^2 = 0.9774$) is slightly higher than that obtained for other equations at 45 °C.

3.5. Kinetic models

The studies of adsorption equilibrium are important in determining the effectiveness of adsorption; however, it is also necessary to identify the types of adsorption mechanism in a given system. In this study we used four different models to predict the adsorption kinetic of phosphate on iron hydroxide-eggshell (pseudo-second-order, Elovich, intra-particle diffusion and Bangham) models. Figs. 8–15 show the plots of the linearized form.

3.5.1. Pseudo-second-order model

Based on equilibrium adsorption, the pseudo-second-order kinetic equation [25] is expressed as

$$\frac{t}{q_t} = \frac{1}{k_2.q_e^2} + \frac{t}{q_e} \quad (7)$$

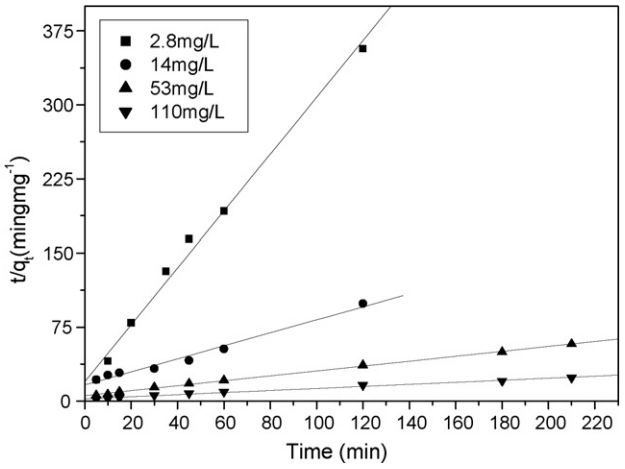

Fig. 8. Pseudo-second-sorption kinetics of phosphate on iron hydroxide-eggshell at various initial concentrations.

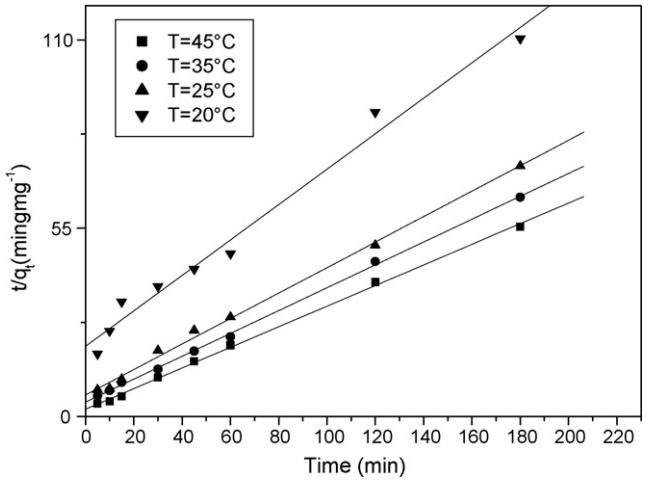

Fig. 9. Pseudo-second-sorption kinetics of phosphate on iron hydroxide-eggshell at various temperatures.

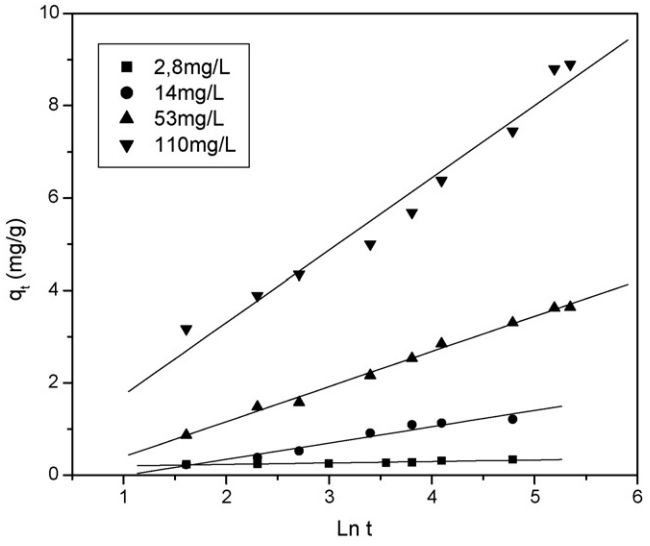

Fig. 10. Elovich plots for phosphate adsorption on iron hydroxide-eggshell at various initial phosphate concentrations.

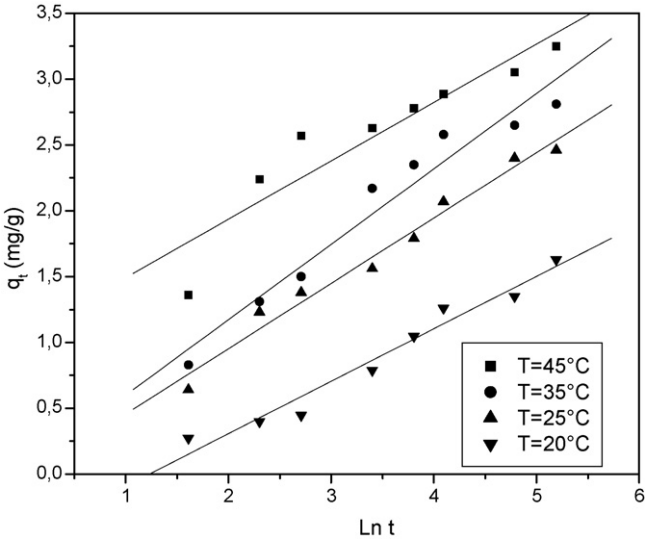

Fig. 11. Elovich plots for phosphate adsorption on iron hydroxide-eggshell at various temperatures.

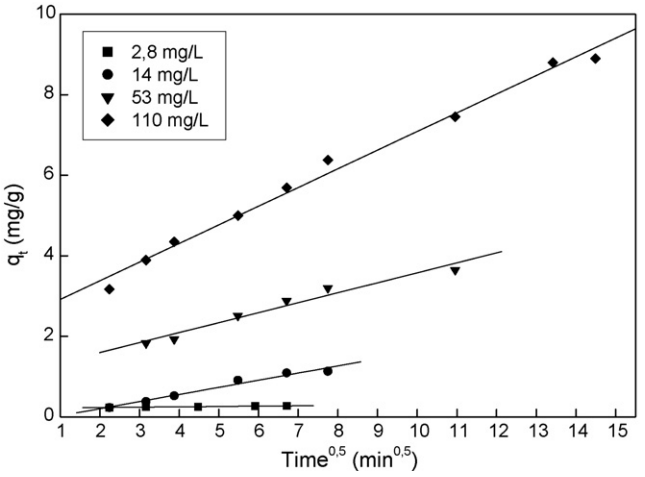

Fig. 12. Plot of intra-particle diffusion modelling of phosphate onto iron hydroxide-eggshell at different initial concentrations.

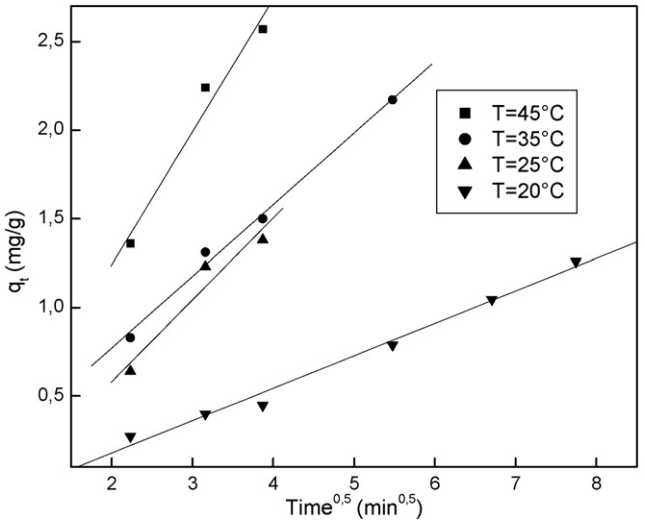

Fig. 13. Plot of intra-particle diffusion modelling of phosphate onto iron hydroxide-eggshell at various temperatures.

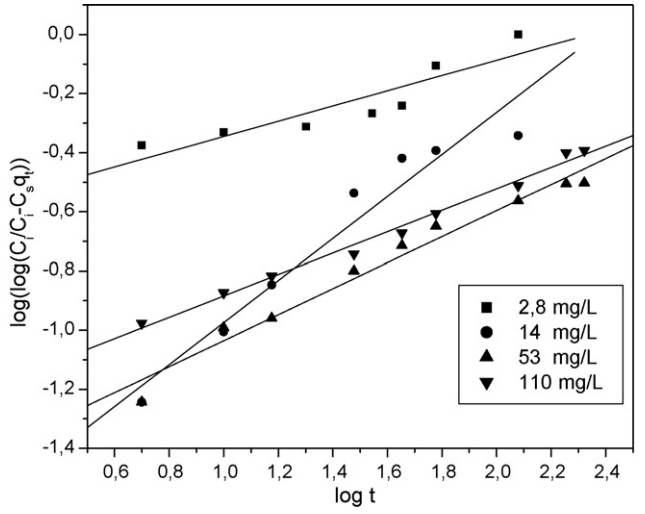

Fig. 14. Bangham's plot for phosphate adsorption on iron hydroxide-eggshell at various initial phosphate concentrations.

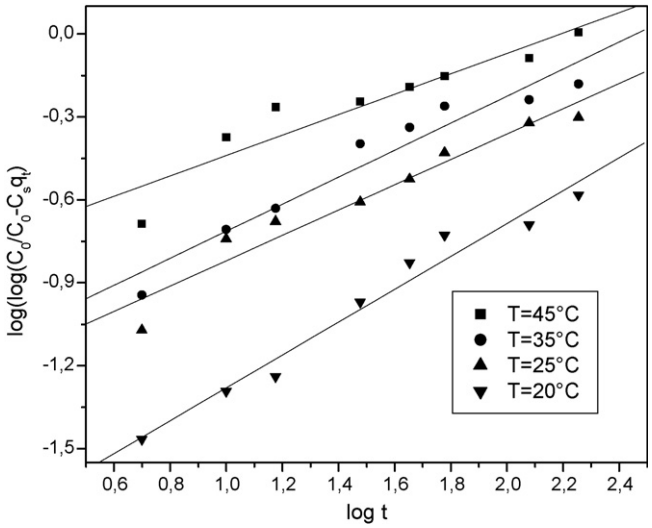

Fig. 15. Bangham's plot for phosphate adsorption on hydroxide-eggshell at various temperatures.

where K_2 is the rate constant of pseudo-second-order adsorption (g/mg min).

The initial adsorption rate, h, (mg/g min) is expressed as

$$h = K_2 q_e^2 \quad (8)$$

The application of the linear form of pseudo-second-order kinetic model on our experimental results is presented in Figs. 8 and 9. Both constants K_2 and h were calculated from the intercept and slope of the line obtained by plotting t/q_t versus t. It can be seen from Table 3 that the kinetics of phosphate adsorption onto iron hydroxide-eggshell follow this model with correlation coefficients higher than 0.987 and the equilibrium adsorption capacity, q_e, increases as the initial phosphate concentration, C_i, increased from 2.8 to 110 mg/L. Further, it was found that the variations of the rate constant, K_2, seem to have a decreasing trend with increasing initial dye concentration.

The variations of t/q_t versus t at various temperatures of the phosphate solution under the initial concentration of 27 mg/L still confirmed to fit the pseudo-second-order model. The values of model parameters (K_2, h and q_e) for different temperatures have been calculated from Eqs. (7) and (8)) and the results are given in Table 3, revealing that the fitted adsorption capacity at equilibrium, q_e, increased with increasing temperature. For example, the values of q_e increased from 1.93 mg/g at 20 °C to 3.32 mg/g at 45 °C. Also, from Table 3, it was noticed that the initial adsorption rate, h, increases with increasing temperature. These results imply that chemisorption mechanism may play an important role for the adsorption of phosphate on the iron hydroxide-eggshell.

Table 3
Parameters for pseudo-second-order equation

	q_{ex} (mg/g)	k_2 (g/mg min)	q_e (mg/g)	h (mg/g min)	r^2
C_i (mg/L)					
2.8	0.355	42.27×10^{-2}	0.347	0.050	0.9918
14	1.450	2.64×10^{-2}	1.517	0.061	0.9824
53	4.900	1.11×10^{-2}	4.010	0.179	0.9978
110	9.400	0.48×10^{-2}	9.570	0.437	0.9873
T (°C)					
45	3.390	4.27×10^{-2}	3.322	0.471	0.9984
35	3.270	2.62×10^{-2}	3.000	0.235	0.9990
25	2.700	2.22×10^{-2}	2.690	0.159	0.9964
20	1.900	1.31×10^{-2}	1.930	0.048	0.9834

Table 4
Parameters for Elovich equation

	a_e (mg/g min)	b_e (g/mg)	r^2
C_i (mg/L)			
2.8	6.46	31.470	0.8567
14	0.126	2.830	0.9545
53	0.472	1.314	0.9947
110	1.751	0.637	0.9668
T (°C)			
45	4.734	2.256	0.8650
35	0.600	1.746	0.9524
25	0.458	2.015	0.9763
20	0.117	2.510	0.9640

3.5.2. Elovich model

Elovich equation is also used successfully to describe second-order kinetic assuming that the actual solid surfaces are energetically heterogeneous, but the equation does not propose any definite mechanism for adsorbate–adsorbent [26]. It has extensively been accepted that the chemisorption process can be described by this semi-empirical equation [27]. The linear form of this equation [26] is given by

$$q_t = \frac{ln\, a_e b_e}{b_e} + \frac{1}{b_e} \ln t \quad (9)$$

where a_e is the initial adsorption rate (mg/g min), and the parameter b_e is related to the extent of surface coverage and activation energy for chemisorption (g/mg).

The Elovich coefficients could be computed from the plots q_t versus $\ln t$. The initial adsorption rate, a_e, and the desorption constant, b_e, were calculated from the intercept and slope of the straight line plots of q_t against $\ln t$ (Figs. 10 and 11). The applicability of the simple Elovich equation for the present kinetic data is generally in agreement with other researcher's results that the Elovich equation was able to describe properly the kinetics of phosphates adsorption on soil and soil minerals [28]. Table 4 lists the kinetic constants obtained from the Elovich equation. It will be seen that the value of a_e and b_e varied as a function of the initial phosphate concentration and solution temperature. Thus, on increasing the initial phosphate concentration from 2.8 to 110 mg/L and the solution temperature from 20 to 35 °C, the value of b_e decreased from 31.47 to 0.638 g/mg and from 2.51 to 1.746 g/mg respectively due to the less available surface for phosphate. On the other hand, an increase in the initial phosphate concentration from 14 to 110 mg/L and solution temperature from 20 to 45 °C leads to an increase in the value of a_e from 0.126 to 1.751 mg/g min and from 0.117 to 4.734 mg/g min respectively. However, these results were not obtained in the initial phosphate concentration range 2.8–14 mg/L and in solution temperature range 35–45 °C and the experimental data did not give a good correlation for low phosphate concentration (2.8 mg/L, $r^2 = 0.8567$) and at temperature of 45 °C ($r^2 = 0.8650$).

3.5.3. Intra-particle diffusion model

The pseudo-second-order and Elovich kinetic models could not identify the diffusion mechanism and the kinetic results were then analyzed by using the intra-particle diffusion model. In the model developed by Weber and Morris [29], McKay and Poots [30], the initial rate of intra-particle diffusion is calculated by linearization of Eq. (10):

$$q_t = K_i t^{1/2} + C \quad (10)$$

where C (mg/g) is the intercept and K_i is the intra-particle diffusion rate constant (mg/g min$^{1/2}$).

According to this model, the plot of uptake, q_t, versus the square root of time ($t^{1/2}$) should be linear if intra-particle diffusion is involved in the adsorption process and if these lines pass through the origin then intra-particle diffusion is the rate-controlling step [29,31]. When the plots do not pass through the origin, this is indicative of some degree of boundary layer control and this further shows that the intra-particle diffusion is not the only rate-limiting step, but also other kinetic models may control the rate of adsorption, all of which may be operating simultaneously.

The intra-particle diffusion, K_i, values were obtained from the slope of the straight line portions of plot of q_t versus $t^{1/2}$ for various phosphate concentrations and solutions temperature (Figs. 12 and 13). The correlation coefficients (r^2) for the intra-particle diffusion model are between 0.9618 and 0.9925 (Table 5). It was observed that intra-particle rate constant values (K_i) increased with initial dye phosphate concentration. The observed increase in K_i values with increasing initial phosphate concentration can be explained by the growing effect of driving force resulted in reducing the diffusion of phosphate species in the boundary layer and enhancing the diffusion in the solid. Also, as shown in Table 5, increasing the temperature promoted the pore diffusion in sorbent particles and resulted in an enhancement in the intra-particle diffusion rate. It is likely that a large number of ions diffuse into the pore before being adsorbed. The corresponding values of intra-particle diffusion rate constant, K_i, for the various concentrations of the phosphate ions (2.8–110 mg/L) and solutions temperatures (20–45 °C) varied from 0.88×10^{-2} to 46.34×10^{-2} mg/g min$^{1/2}$ and from 18.32×10^{-2} to 74.96×10^{-2} mg/g min$^{1/2}$ respectively (Table 5). From Figs. 12 and 13, it can be observed that the straight lines did not pass through the origin and this further indicates that the intra-particle diffusion is not the only rate-controlling step.

Also, the diffusion coefficients for the intra-particle transport of phosphate species within the pores of iron hydroxide-eggshell particles have been calculated by employing Eqs. (11) and (12) [32].

$$D_i = \frac{0.03 \times r^2}{t_{1/2}} \quad (11)$$

$$t_{1/2} = \frac{1}{K q_e} \quad (12)$$

where D_i is the diffusion coefficient with the unit cm^2/s; $t_{1/2}$ is the time (s) for half-adsorption of phosphate species and r is the average radius of the adsorbent particle in cm. The value of r (average radius) was calculated as 67×10^{-4} cm. In these calculations, it has been assumed that the solid phase consists of spherical particles.

The diffusion coefficients varied from 0.056×10^{-8} to 0.318×10^{-8} cm^2/s with an increase of solution temperature from 20 to 45 °C. At higher temperatures the attraction between the functional groups waste iron hydroxide-eggshell and phosphate species gets stronger. The values of the internal diffusion coefficient, D_i, shown in Table 5 fell well within the magnitudes reported in literature [33], specifically for chemisorption system

Table 5
Parameters for intra-particle diffusion model

	Intra-particle diffusion			
	K_i (mg/g min$^{1/2}$)	r^2	D_i (cm^2/s)	$t_{1/2}$ (min)
C_i (mg/L				
2.8	0.88×10^{-2}	0.9723	0.33×10^{-8}	6.82
14	17.69×10^{-2}	0.9723	0.090×10^{-8}	24.97
53	24.75×10^{-2}	0.9618	0.100×10^{-8}	22.47
110	46.34×10^{-2}	0.9903	0.103×10^{-8}	21.77
T (°C)				
45	74.96×10^{-2}	0.9903	0.318×10^{-8}	7.05
35	46.12×10^{-2}	0.9364	0.176×10^{-8}	12.72
25	40.41×10^{-2}	0.9925	0.133×10^{-8}	16.74
20	18.32×10^{-2}	0.9875	0.056×10^{-8}	39.50

(10^{-5} to 10^{-13} cm^2/s), it is also observed that the diffusion coefficient, D_i, decreased from 0.33×10^{-8} to 0.09×10^{-8} cm^2/s as initial phosphate concentration increased from 2.8 to 14 mg/L. This behaviour of concentration dependent diffusivity agrees with literature works [34]. The corresponding diffusion coefficients of the phosphate for 53–110 mg/L concentration range were not affected with changes of initial phosphate concentration.

Kinetic data can further be used to check whether pore diffusion is the only rate-controlling step or not in the adsorption system by using Bangham's equation.

3.5.4. Bangham's model

Bangham's model [35] equation is generally expressed as

$$\log \log \left[\frac{C_i}{C_i - C_s q_t}\right] = \log \left[\frac{k_b C_s}{2.303V}\right] + \alpha \log t \quad (13)$$

where C_i is the initial concentration of the adsorbate in solution (mg/L), V the volume of the solution (mL), C_s the weight of adsorbent used per liter of solution (g/L), q_t (mg/g) the amount of adsorbate retained at time t, α (<1) and k_b are constants. $\log \log[C_i/C_i - C_s q_t]$ was plotted against $\log t$. The phosphate adsorption fits the Bangham's model. α and k_b constants were calculated from the intercept and slope of the straight line plots of $\log \log[C_i/C_i - C_s q_t]$ against $\log t$ (Figs. 14 and 15). If the experimental data is represented by this equation then the adsorption kinetics are limited by the pore diffusion [36].

Table 6 lists the kinetic constants obtained from the Bangham's equation. It will be seen that the value of α and k_0 varied as a function of the initial phosphate concentration, C_i, and solution temperature. Thus, on increasing the temperature from 20 to 45 °C, the value of α decreased from 0.37 to 0.59 and the value of k_b increased from 47.70 to 4.10 (mL/g/L). The experimental data did not give a good correlation for low initial phosphate concentration (C_i = 2.8 mg/L, r^2 = 0.8300) and at 45 °C (r^2 = 0.8791). In addition, it was found that the correlation coefficients for the Elovich model are higher than those obtained for Bangham's model. This result still confirmed that the pore diffusion is not the only rate-controlling step.

3.6. Thermodynamic parameters

The thermodynamic parameters of the adsorption process were determined from the experimental data obtained using the following equations [37]:

$$\Delta G^\circ = -RT \ln K_d \quad (14)$$

$$\ln K_d = -\frac{\Delta H^\circ}{RT} + \frac{\Delta S^\circ}{R} \quad (15)$$

$$K_2 = K_0 e^{[-E_a/RT]} \quad (16)$$

Table 6
Parameters for Bangham's equation

	Bangham's model		
	k_b (mL/g/L)	α	r^2
C_i (mg/L)			
2.8	76.55	0.26	0.8300
14	6.34	0.71	0.9445
53	10.30	0.44	0.9721
110	17.40	0.36	0.9721
T (°C)			
45	47.70	0.37	0.8791
35	19.27	0.49	0.9381
25	16.20	0.46	0.9393
20	4.10	0.59	0.9695

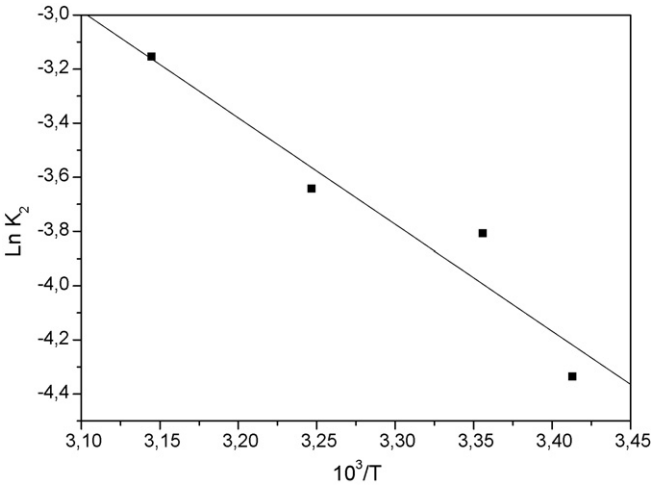

Fig. 16. Arrhenius plots for the adsorption of phosphate onto iron hydroxide-eggshell at various temperatures.

where K_d is the distribution coefficient for the adsorption, ΔS°, ΔH° and ΔG° are the change of entropy, enthalpy and the Gibbs energy, T is the absolute temperature, R is the gas constant. The second-order rate constant is expressed as a function of temperature by the Arrhenius equation (Eq. (16)). K_0 is the temperature independent factor (g/mg min), E_a is the activation energy of sorption (kJ/mol). Fig. 16 shows a linear relationship between the logarithm of rate constant and the reciprocal of temperature. The values of ΔH (81.84 kJ) and ΔS (0.282 kJ/mol) were determined from the slope and intercept of the plot of $\ln K_d$ versus $1/T$ (Fig. 17). The ΔH° and ΔS° values are positive. The positive values of E_a (32.74 kJ/mol) and ΔH indicate the presence of an energy barrier in the adsorption and endothermic process [37]. Lazaridis and Asouhidou [38] stated that in a diffusion-controlled process, the activation energy of adsorption was less than 25–30 kJ/mol; based on the results of activation energy and intra-particle model, this study proposed that the adsorption involved intra-particle diffusion that was not the only rate-controlling step and the other kinetic models might control the adsorption rate [39]. The positive value of entropy change (ΔS) reflects good affinity of phosphate ions towards the sorbent and the increasing randomness at the solid-solution interface during the adsorption process [40]. The negative values of ΔG° (Eq.

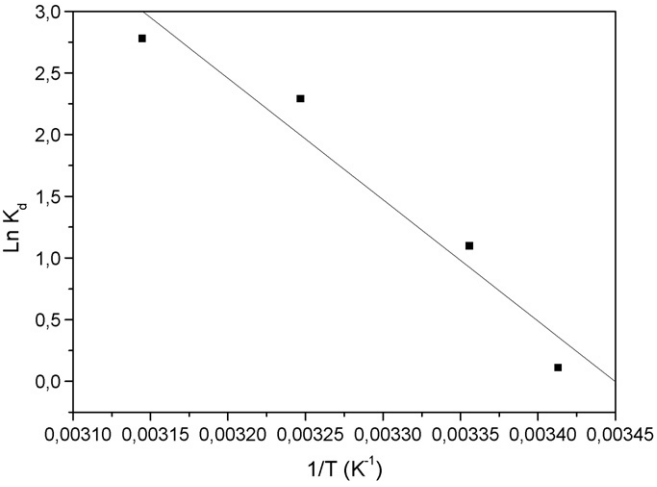

Fig. 17. Van't Hoff plot for the adsorption of phosphate species onto iron hydroxide-eggshell at various temperatures.

Table 7
Thermodynamic parameters

Temperature (°C)	$-\Delta G$ (kJ/mol)	$T\Delta S$ (kJ/mol)	ΔH (kJ/mol)
20	0.2651	82.72	81.84
25	2.662	84.13	
35	5.745	86.95	
45	7.194	89.78	

Table 8
Reported sorption capacity (q_m) of phosphate for some low-cost adsorbents

q (mg/g)	
Macrophyte (*Hydrilla verticillata*)	0.286 [18]
Goethite	6.42 [41]
Natural zeolite	2.15 [42]
Na-natural zeolite	2.19 [43]
Iron oxide tailings	8.21 [13]
SCS (synthetic iron oxide coated sand)	1.5 [44]
CB (coated crushed brick)	1.75 [44]
NC S (naturally iron oxide coated sand)	0.88 [44]
Iron-hydroxide eggshell	14.49 our study

(12)) reflect that the adsorption of phosphate onto iron hydroxide-eggshell is feasible and spontaneous. The ΔG° value decreases from −0.2651 to −7.194 kJ/mol when the temperature increases from 20 to 45 °C (Table 7), suggesting the more adsorbable of phosphate species with increasing temperature.

4. Conclusion

The experimental results showed that iron hydroxide-eggshell could potentially be employed as a sorbent in the removal of phosphate ions.

The kinetics of phosphate sorption by waste material were fast, reaching 73% of the total adsorption capacity in 30 min (T = 45 °C, pH 7, C_i = 27 mg/L). Adsorption phosphate was highly temperature-dependent. The Freundlich, Langmuir and Langmuir–Freundlich adsorption models were used for the mathematical description of the adsorption equilibrium of phosphate species by iron hydroxide-eggshell. A pseudo-second-order model was applied to the experimental data, the values of K_2, h and q_e all increased with the temperature, suggesting that increasing the temperature increased the adsorption capacity and the adsorption rate. Also, it was observed that the intra-particle diffusion was not the only rate-controlling step. Positive ΔH° and ΔS° values indicated that the adsorption of phosphate onto iron hydroxide-eggshell was endothermic. This result was supported by the increasing adsorption of phosphate ion with temperature. To illustrate the potential in the use of iron hydroxide-eggshell in actual applications, a comparative evaluation of the adsorptions capacities of various types of low-cost adsorbents for the sorption of phosphates species is provided in Table 8. This comparison clearly indicated that iron hydroxide-eggshell is an effective adsorbent for phosphate removal.

References

[1] G. Tchobanoglus, F.L. Burton, Wastewater Engineering, MC Graw-Hill Inc., 1991.
[2] D.G. Grubb, M.S. Guimaraes, R. Valencia, Phosphate immobilization using acidic type F fly ash, J. Hazard. Mater. 76 (2–15) (2000) 217–236.
[3] G. Akay, B. Keskinler, A. Cakici, U. Danis, Phosphate removal from water by red mud using crossflow microfiltration, Water Res. 32 (3) (1998) 717–726.
[4] A. Ugurlu, B. Salman, Phosphorus removal by fly ash, Environ. Int. 24 (8) (1998) 911–918.
[5] E. Galameau, R. Gehr, Phosphorus removal from wastewaters: experimental and theoretical support for alternative mechanisms, Water Res. 31 (2) (1997) 328–338.
[6] L. Chang-Jun, L. Yan-Zhong, L. Zhao-Kun, C. Zhao-Yang, Z. Zhong-Guo, J.I.A. Zhi-Ping, Adsorption removal of phosphate from aqueous solution by actived red mud, J. Environ. Sci. 19 (10) (2007) 1166–1170.
[7] E. Oguz, Sorption of phosphate from solid/liquid interface by fly ash, Colloid Surf. Physicochem. Eng. Aspects 262 (1–3) (2005) 113–117.
[8] L. Johanson, J.P. Gustafsson, Phosphate removal using blast furnace slags and opoka-mechanisms, Water Res. 34 (1) (2000) 259–265.
[9] S. Huang, B. Chiswell, Phosphates removal from waste-water using spent alum sludge, Water Sci. Technol. 42 (3–4) (2000) 295–300.
[10] E.E. Codling, R.L. Chaney, C.L. Mulchi, Use of aluminium and iron-rich residues to immobilize phosphorus in poultry litter and litter-amended soils, J. Environ. Qual. 29 (6) (2000) 1924–1931.
[11] W. Yujiro, Y. Hirohisa, K. Takeshi, T. Junzo, K. Yu, M. Yusuke, Adsorption behavior of phosphorus on synthetic boehmites, in: Proceedings of the 19th International Japan-Korea Seminar on Ceramics, 2002, pp. 80–84.
[12] K. Karageorgiou, M. Paschalis, G.N. Anastassakis, Removal of phosphate species from solution by adsorption onto calcite used natural adsorbent, J. Hazard. Mater. 139 (3) (2007) 447–452.
[13] L. Zeng, X. Li, J. Liu, Adsorptive removal of phosphate from aqueous solutions using iron oxide tailings, Water Res. 38 (5) (2004) 1318–1326.
[14] R.D. Van der Weijden, R.N.J. Comans, Sorption and sorption reversibility of cadmium on calcite in the presence of phosphates and sulfates, Mar. Chem. 57 (1–2) (1997) 119–132.
[15] D. Wenming, G. Zhijun, D. Jinzhou, Z. Liying, T. Zuji, Sorption characteristics of zinc(II) by calcareous soil-radiotracer study, Appl. Radiat. Isotopes 54 (3) (2001) 371–375.
[16] N. Yeddou, A. Bensmaili, Equilibrium and kinetic modelling of iron adsorption by eggshells in a batch system: effect of temperature, Desalination 206 (1–3) (2007) 127–134.
[17] APHA (American Public Health Association) (1992).
[18] S. Wang, X. Jin, H. Zhao, F. Wu, Phosphate biosorption characteristics of a submerged macrophyte *Hydrilla verticillata*, Aqua. Bot. 89 (1) (2008) 23–26.
[19] M. Yalvac Can, E. Yildiz, Phosphate removal from water by fly ash: factorial experimental design, J. Hazard. Mater. B 135 (1–3) (2006) 165–170.
[20] L. Yanzhong, L. Changjun, L. Zhaokun, P. Xianjia, Z. Chunlei, C. Zhaoyang, Z. Zhongguo, F. Jinghua, J. Zhiping, Phosphate removal from aqueous solutions using raw and activated red mud and fly ash, J. Hazard. Mater. B137 (1) (2006) 374–383.
[21] I. Langmuir, The adsorption of gases on plane surfaces of glass, mica, and platinum, J. Am. Chem. Soc. 40 (1918) 1361–1368.
[22] H. Freundlich, Adsorption in solution, Phys. Chem. Soc. 40 (1906) 1361–1368.
[23] R. Sips, On the structure of a catalyst surface, J. Chem. Phys. 16 (5) (1948) 490–495.
[24] M.M. Dávila-Jimenez, M.P. Elizalde-Gonzalez, A.A. Peláez-Cid, Adsorption interaction between natural adsorbents and textile dyes in aqueous solution, Colloid Int. Sci. A 254 (1–3) (2005) 107–114.
[25] Y.S. Ho, Review of second order models for adsorption systems, J. Hazard. Mater. B136 (3) (2006) 681–689.
[26] D.L. Sparks, Kinetics of Soil Chemical Processes, Academic Press Inc., New York, 1989.
[27] J. Zhang, R. Stanforth, Slow adsorption reaction between arsenic species and Goethite (α-FeOOH): diffusion or heterogeneous surface reaction control, Langmuir 21 (2005) 2895–2901.
[28] S.H. Chien, W.R. Clayton, Application of Elovich equation to the kinetics of phosphate release and sorption in soils, Soil Sci. Soc. Am. J. 44 (1980) 265–268.
[29] W.J. Weber, J.C. Morris, Kinetics of adsorption on carbon from solution, J. Sanit. Eng. Div. Am. Soc. Civ. Eng. 89 (1963) 31–60.
[30] G. Mckay, V.J.P. Poots, Kinetics and diffusion process in colour removal from effluent using wood as an adsorbent, J. Chem. Technol. Biotechnol. 30 (1980) 279–292.
[31] M. Arami, N. Yousefi Limaee, N.M. Mahmoodi, Evaluation of the adsorption kinetics and equilibrium for the potential removal of acid dyes using a biosorbent, Chem. Eng. J. 139 (1) (2008) 2–10.
[32] A.K. Bhattacharya, C. Venkobar, Removal of cadmium by low cost adsorbents, J. Environ. Eng. 110 (1) (1984) 110–122.
[33] D. Chatzopoulos, A. Varma, R.L. Irvine, Activated carbon adsorption and desorption of toluene in the aqueous phase, AIChE J. 39 (1993) 2027–2041.
[34] G.M. Walker, L. Hansen, J.A. Hanna, S.J. Allen, Kinetics of a reactive dye adsorption onto dolomic sorbents, Water Res. 37 (9) (2003) 2081–2089.
[35] A. Bhatnagar, A.K. Jain, A comparative adsorption study with different industrial wastes as adsorbents for the removal of cationic dyes from water, Colloid Int. Sci. 281 (1) (2005) 49–55.
[36] E. Tutem, R. Apak, C.F. Unal, Adsorptive removal of chlorophenols from water by bituminous shale, Water Res. 32 (8) (1998) 2315–2324.
[37] B.H. HAmeed, A.A. Ahmad, N. Aziz, Isotherms, kinetics and thermodynamics of acid dye adsorption on activated palm ash, Chem. Eng. J. 133 (1–3) (2007) 195–203.
[38] N.K. Lazaridis, D.D. Asouhidou, Kinetics of sorptive removal of chromium (VI) from aqueous solutions by calcined Mg-Al-CO_3 hydrotalcite, Water Res. 37 (12) (2003) 2875–2882.
[39] W. Chung-Hsin, Adsorption of reactive dye onto carbon nanotubes: equilibrium, kinetics and thermodynamics, J. Hazard. Mater. 144 (1–2) (2007) 93–100.
[40] S. Senthilkumaar, P. Kalaamani, C.V. Subburaam, Liquid phase adsorption of crystal violet onto activated carbons derived from male flowers of coconut tree, J. Hazard. Mater. B 136 (3) (2006) 800–808.

[41] O.K. Borggaard, B. Raben-Lange, A.L. Gimsing, B.W. Strobel, Influence of humic substances on phosphate adsorption by aluminium and iron oxides, Geoderma 127 (3–4) (2005) 270–279.
[42] K. Sakadevan, H.J. Bavor, Phosphate adsorption characteristics of soils, slags and zeolite to be used as substrates in constructed wetland systems, Water Res. 32 (2) (1998) 393–399.
[43] D. Wu, B. Zhang, C. Li, Z. Zhang, H. Kong, Simultaneous removal of ammonium and phosphate by zeolite synthesized from fly ash as influenced by salt treatment, Colloid Int. Sci. 304 (2) (2006) 300–306.
[44] N. Boujelben, J. Bouzid, Z. Elouear, M. Feki, F. Jamoussi, A. Montiel, Phosphorus removal from aqueous solution using iron coated natural and engineered sorbents, J. Hazard. Mater. 151 (1) (2008) 103–110.